

Effects of atomic and magnetic order on electronic transport in Pd-rich Pd-Fe alloys

J. Kudrnovský and V. Drchal

Institute of Physics, Academy of Sciences of the Czech Republic, Na Slovance 2, CZ-182 21 Praha 8, Czech Republic

S. Khmelevskiy

CMS, Institute of Applied Physics, Vienna University of Technology, Gußhausstrasse 25a, Makartvilla, AT-1020, Vienna, Austria

I. Turek

Institute of Physics of Materials, Academy of Sciences of the Czech Republic, Žitkova 22, CZ-616 62 Brno, Czech Republic

(Received 1 September 2011; revised manuscript received 9 December 2011; published 27 December 2011)

The transport properties of Pd-rich PdFe alloys are investigated as a function of the atomic and magnetic order on the $L2_1$ (Cu_3Au) lattice. The residual resistivity, anisotropic magnetoresistance (AMR), and anomalous Hall effect are calculated from first principles in their dependence on the degree of atomic order. The calculations are based on the relativistic generalization of the transport Kubo-Greenwood approach as formulated in the framework of the first-principles tight-binding linear muffin-tin orbital (TB-LMTO) method and coherent potential approximation (CPA). The effect of the thermal magnetic disorder on the resistivity (thermal magnetoresistance) and AMR has been also studied using the disordered local moment approach based on the CPA. It is found that the experimentally observed fast decrease of AMR ratio with temperature can be mostly ascribed to the spin disorder effects. Our results are in an overall good agreement with available experimental data.

DOI: [10.1103/PhysRevB.84.214436](https://doi.org/10.1103/PhysRevB.84.214436)

PACS number(s): 71.15.Mb, 71.15.Rf, 71.23.-k, 72.10.Fk

I. INTRODUCTION

The residual resistivity in metallic alloys is one of the important indications of substitutional atomic disorder and has been a subject of intensive experimental and theoretical studies.¹ At zero temperature magnetically ordered random alloys exhibit anisotropy of the resistivity in the applied magnetic field due to spin-orbit coupling effects, the so-called anisotropic magnetoresistance (AMR) which attracts a considerable interest also from the point of view of technological applications. Progress has been achieved in calculations of the residual resistivities and AMR effects from *ab initio* theories based on the local spin-density approximation (LSDA)² in the last decade. In particular, for substitutionally disordered Fe-Ni permalloy alloys the zero temperature AMR ratio has been calculated in a good agreement with experiment.^{3,4} However, the residual resistivity due to substitutional disorder is strongly dependent on the degree of disorder present in the alloy of the same atomic composition (vanishing in the ideally ordered compound) which depends on the thermal history of the sample.⁵ The AMR ratio as well depends on the degree of disorder, but in a less obvious way. This interesting problem has not received up to now much attention from the theoretical point of view. To fill this gap we have undertaken a thorough first-principles investigation of the effects of partial order on residual resistivity and magnetotransport properties choosing as a case study Pd-rich Fe-Pd alloys, where degree of partial order can be relatively easily controlled by annealing procedure and corresponding data on resistivity exists in literature.⁶

The AMR ratio in cubic systems is usually defined as $(\rho_{zz} - \rho_{xx})/\rho_0$, where $\rho_{xx} = \rho_{yy}$ and ρ_{zz} are diagonal components of the resistivity tensor in the magnetic field pointing along the z direction and $\rho_0 = (2\rho_{xx} + \rho_{zz})/3$ is the isotropic residual resistivity. One important property of the AMR in alloys is a fast decrease of the AMR ratio with temperature, which

is a very unwanted feature for applications. For instance, the AMR values at low temperature reach 18% in Ni-rich fcc-NiFe alloys and this value decreases to 5% at room temperature. In the Pd-rich PdFe alloys investigated here the AMR at low temperatures can reach values up to 10%, but it decreases well below 1% at room temperatures.⁶ It should be noted that much larger values of the magnetoresistivity can be obtained for artificially prepared metallic multilayers (the so-called giant magnetoresistance). Authors of Ref. 6 have investigated the dependence of magnetotransport on the amount of disorder in the system by using samples with different thermal treatments. The most important findings were: (i) the sample with higher order has a smaller total resistivity; (ii) the AMR is larger in nonstoichiometric $\text{Pd}_{70}\text{Fe}_{30}$ alloy as compared to stoichiometric Pd_3Fe alloy; (iii) various amount of order influences the AMR values only weakly in the stoichiometric samples, but it leads to a pronounced increase of the AMR with order in the nonstoichiometric samples; and (iv) the resistivity increases with increasing temperature while the AMR values are reduced to a small fraction of their values at room temperature.⁶ Authors ascribed this reduction to phonon scattering which exceeds the impurity scattering at room temperature, but the discussion of the influence of the spin disorder was omitted and we will show that it plays an important role. Moreover, our results show that the spin disorder effects alone may be responsible for the experimentally observed fast decrease of the AMR ratio with temperature.

The two mechanisms of scattering responsible for the resistivity of magnetic metals are effective at finite temperatures, namely the scattering on phonons and on magnons. With exception of very low temperatures, the phonon part of the resistivity increases with temperature linearly.⁷ The dependence of the resistivity on magnon scattering, the so-called spin disorder,⁸ is quite difficult to describe theoretically and it is still a challenge for the first-principles modeling.

Below we utilize a model of the spin disorder based on the uncompensated disordered local moment (DLM)⁹ picture which will allow us to discuss the influence of temperature on the magnetotransport properties from first principles. We will also discuss the dependence of the anomalous Hall effect (AHE) on the order in Pd-rich PdFe alloys despite the fact that no experimental data are available.

Another aspect of the present work is a detailed study of the relation of the atomic order with residual resistivity and magnetoresistance for Pd-rich PdFe alloys (L₂₁ structure) in which exists some kind of antisite Pd-Fe disorder even at the stoichiometric composition. The correlation of calculated magnetotransport properties with the degree of chemical order in the system may represent an additional possibility to characterize the amount of order, complementary to conventional methods based on the x-ray and neutron-scattering experiments. We wish to mention related studies in which the effect of the long-range⁵ or short-range¹⁰ orders on the resistivity was studied for nonmagnetic alloys and in the case of Ref. 5 neglecting also the spin-orbit effects.

II. FORMALISM

The ordered Pd₃Fe alloy crystallizes in the Cu₃Au-lattice structure (L₂₁) which can be imagined as four interpenetrating simple-cubic sublattices of which three are occupied by Pd atoms and one by Fe atoms. Together they form a network of fcc-lattice sites in which the nearest-neighbor distance is that among Pd and Fe atoms, that is, each Fe atom has as its nearest neighbors Pd atoms.

Different thermal treatment leads to a different amount of disorder in the system, which is present even in the stoichiometric Pd₃Fe alloy. We characterize the amount of disorder by the concentration of antisite Fe atoms on Pd sublattices $x_{\text{Fe}[\text{Pd}]}$. If $x_{\text{Fe}[\text{Pd}]} = 0$, the system is an ideal ordered Pd₃Fe alloy, in the limit $x_{\text{Fe}[\text{Pd}]} = 0.25$ we recover a completely disordered fcc-Pd₇₅Fe₂₅ alloy. The nonstoichiometric Pd-rich alloys, for example, Pd₇₀Fe₃₀, cannot possess full order. We choose as the most ordered system the one with fully occupied Fe sublattice and with the rest of the Fe atoms distributed randomly on three Pd sublattices with the same concentrations on each sublattice. The disorder is then characterized by the concentration of Pd atoms on the Fe sublattice $x_{\text{Pd}[\text{Fe}]}$. Consequently, a completely disordered Pd₇₀Fe₃₀ alloy corresponds to $x_{\text{Pd}} = 0.7$ on each sublattice.

The experimental lattice constant of the ordered Pd₃Fe alloy ($a = 3.849$ Å) corresponding to the Wigner-Seitz radius $R_{\text{WS}} = 2.843$ a.u. was used for all studied alloys. We thus neglect possible small variations of the lattice constant due to disorder, chemical composition, and the temperature as our main concern is the chemical ordering in the system.

The electronic structure calculations were performed in the framework of the tight-binding linear muffin-tin orbital (TB-LMTO) basis¹¹ and the density functional theory (DFT) as formulated in terms of the Green function approach. This approach is necessary in order to include the effect of substitutional disorder due to a possible presence of the Pd-Fe swapping. The effect of substitutional disorder in the system was described by the coherent potential approximation (CPA).¹² The local spin-density approximation (LSDA) for

the exchange-correlation part of the potential was used. The calculations employed the s, p, d basis, the same atomic radii were adopted for all atoms, and the Vosko-Wilk-Nusair exchange-correlation potential¹³ was used. Relativistic corrections were included approximately by adding the on-site spin-orbit coupling term to the scalar-relativistic TB-LMTO Hamiltonian and treating it as a perturbation in the sense that the calculated spin-up and spin-down charge densities enter the conventional LSDA solver.¹⁴ The value of the spin-orbit coupling was determined self-consistently during calculations.

An early first-principles formulation of the spin-polarized relativistic transport using the KKR-CPA method,³ in particular as it concerns the evaluation of the AHE, was incorrect. A correct formulation of the linear-response theory in both Dirac and weak-relativistic (spin-orbit) approaches, based on the Kubo-Sředa formula, was developed in Ref. 15. Its first-principles implementation in the framework of the fully relativistic KKR-CPA approach has appeared recently¹⁶ and the present formulation is very similar to it. Specifically, we employ the TB-LMTO-CPA method including the spin-orbit term. The formalism for diagonal elements of the resistivity tensor was published recently,¹⁷ while full details of the formalism can be found in Ref. 18. In addition to the treatment of relativistic corrections in the framework of the spin-orbit approach, the present implementation employs a nonrandom velocity operator formulation.¹⁹ This has some advantages over the conventional KKR-CPA approach¹⁶ in which the velocity operator is a random quantity.

The conductivity tensor $\tilde{\sigma}$ for cubic systems in the TB-LMTO method is

$$\sigma^{\mu\nu} \propto \text{Tr}\{v^\mu(g_+^\alpha - g_-^\alpha)v^\nu g_-^\alpha - v^\mu g_+ v^\nu(g_+^\alpha - g_-^\alpha)\} + i \text{Tr}\{(X^\mu v^\nu - X^\nu v^\mu)(g_+^\alpha - g_-^\alpha)\}, \quad (1)$$

where $g_\pm^\alpha = g^\alpha(E_F \pm i\delta)$ is the Green function matrix, δ is an infinitesimal number, and $v^\mu = -i[X^\mu, S^\alpha]$ is the nonrandom effective velocity operator. In the above expression S^α is the structure constant of the TB-LMTO theory, E_F is the Fermi energy, X^μ is the coordinate of the lattice site, the symbol α denotes the screened LMTO representation, and Tr denotes the trace taken over the lattice sites (X), orbital (L), and spin moment (s) subspaces. The disorder-induced vertex corrections are included in the framework of the CPA.²⁰ Finally, the resistivity and conductivity tensors are related by a simple relation $\tilde{\rho} = \tilde{\sigma}^{-1}$. Calculations were done assuming an imaginary part of the complex energy δ [see Eq. (1)] equal to 10^{-5} Ry. A large number of points in the Brillouin zone (BZ) (several millions points in the full BZ) were used to obtain well-converged results.

Once the components of the resistivity tensor are calculated, the total resistivity ρ_0 and the AMR ratio can be determined. In the present approach we employ a closely related definition of the AMR, namely $\text{AMR} = (\rho_{zz} - \rho_{xx})/\rho_{zz}$. The AHE is given by the off-diagonal element σ_{xy} of the conductivity tensor. According to Ref. 16 we can roughly separate out the *intrinsic* and *extrinsic* parts of the AHE. The former one is due to the coherent part of σ_{xy} (vertex corrections are neglected), while the latter one can be identified with the vertex part of σ_{xy} . The vertex part is thus simply a difference between full and coherent parts of the AHE. Such identification is justified by

the fact that the *intrinsic* part of the AHE exists even in perfect systems without any disorder and it is determined only by the band structure, spin-orbit coupling, and exchange splitting. The coherent part of the AHE in disordered metals differs from that of pure metals by substituting the δ -function-like spectral densities of pure metals by broadened Lorentzian-like spectral densities in disordered metals and this part of the AHE is thus weakly concentration dependent. On the other hand, vertex corrections are zero in a nonrandom system and are strongly dependent on the impurity concentration so that they can be roughly identified with skew-scattering contribution to the AHE. Finally, we will also briefly discuss a simple model of the spin disorder and how it influences magnetotransport properties. The model we have in mind is an uncompensated DLM approach.

III. RESULTS AND DISCUSSION

In this section we present results of the theoretical modeling and compare them with available experimental data. In the next subsection we discuss the influence of the disorder on the ground state electronic structure and magnetic properties of Pd-Fe alloys. Then we discuss our results concerning residual resistivity and AMR and their dependence on the degree of the chemical long-range order. The temperature effects on the AMR ratio is the subject of study in third subsection, and we conclude this section by presenting results related to the AHE.

A. Electronic and magnetic structure

We present the relativistic nonmagnetic density of states (DOS) and its decomposition into contributions from Pd and Fe sublattices in Fig. 1. A high value of the total DOS at the Fermi energy clearly indicates (Stoner criterion) the instability of the nonmagnetic state with respect to formation of the ferromagnetic state. The most important contribution is due

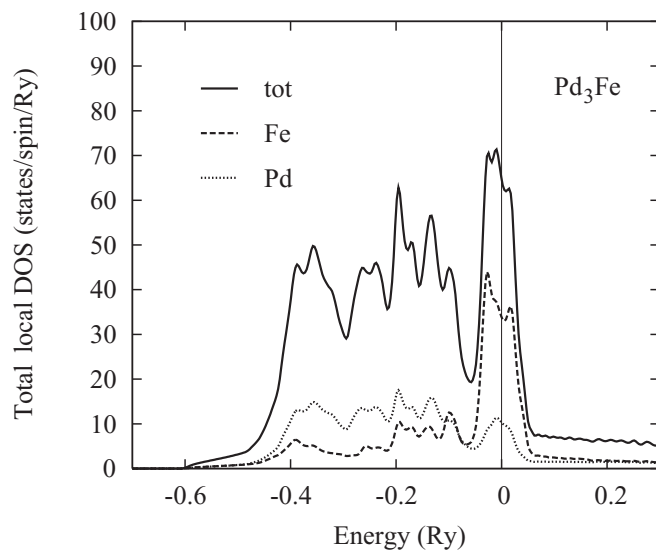


FIG. 1. The relativistic nonmagnetic total and component resolved densities of states for ideal ordered Pd₃Fe alloy. The Fermi energy is set to zero.

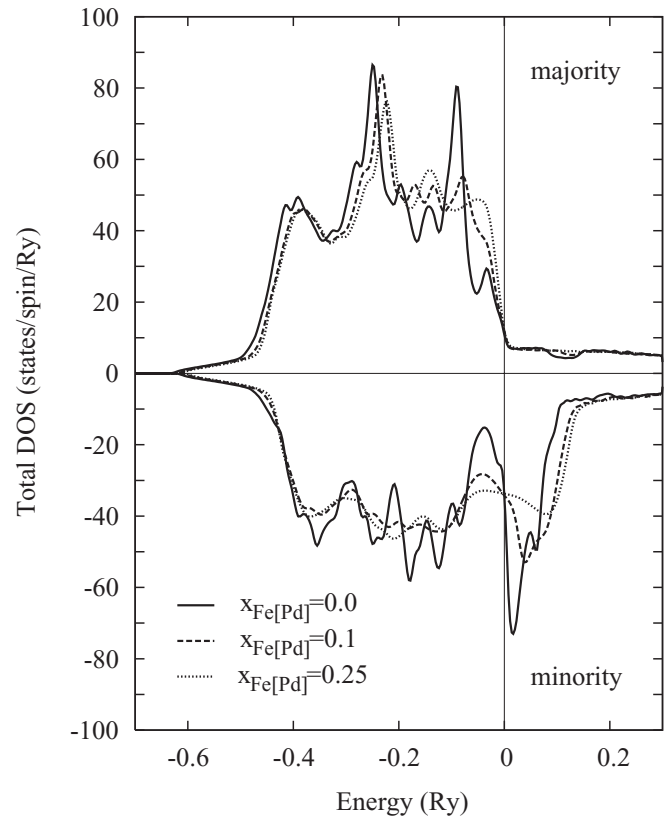


FIG. 2. The relativistic spin-resolved ferromagnetic total densities of states for three different values of antisite concentrations $x_{\text{Fe}[\text{Pd}]}$ of Fe atoms on Pd sublattices in Pd₃Fe alloy. The case $x_{\text{Fe}[\text{Pd}]} = 0$ corresponds to an ideal Pd₃Fe alloy while the case $x_{\text{Fe}[\text{Pd}]} = 0.25$ corresponds to a completely disordered fcc-Pd₇₅Fe₂₅ alloy. The Fermi energy is set to zero.

to Fe atoms, but there is also a small peak in the Pd-local DOS at the Fermi energy induced by Fe-Pd hybridization.

The total DOS of the ferromagnetic Pd₃Fe alloy with increasing influence of Fe-antisite disorder is shown in Fig. 2. The effect of disorder is largest in the energy region around the Fermi energy, slightly below (above) it for majority (minority) states and the disorder is in general stronger for minority states. Present results for Pd₃Fe alloy in both ordered and fully disordered phases agree reasonably well with a previous study²¹ in which self-consistent potentials of the ordered phase were used also for the disordered phase. Small differences can be ascribed to this approximation and to the neglect of relativistic corrections in previous calculations.

Pd₃Fe and Pd₇₀Fe₃₀ alloys differ by their electron concentrations and different behavior of electronic states at the Fermi energy (transport relaxation time and velocities) which both influence transport properties. To illustrate this point, we present in Fig. 3 the total densities for the most ordered and fully disordered phases around the Fermi energy. Although the general trend is similar due to similar compositions, the differences are seen, in particular for minority bands. These differences are a precursor of different transport behavior as we shall see below.

The dependence of total and local Fe- and Pd-magnetic moments as a function of antisite concentrations are shown

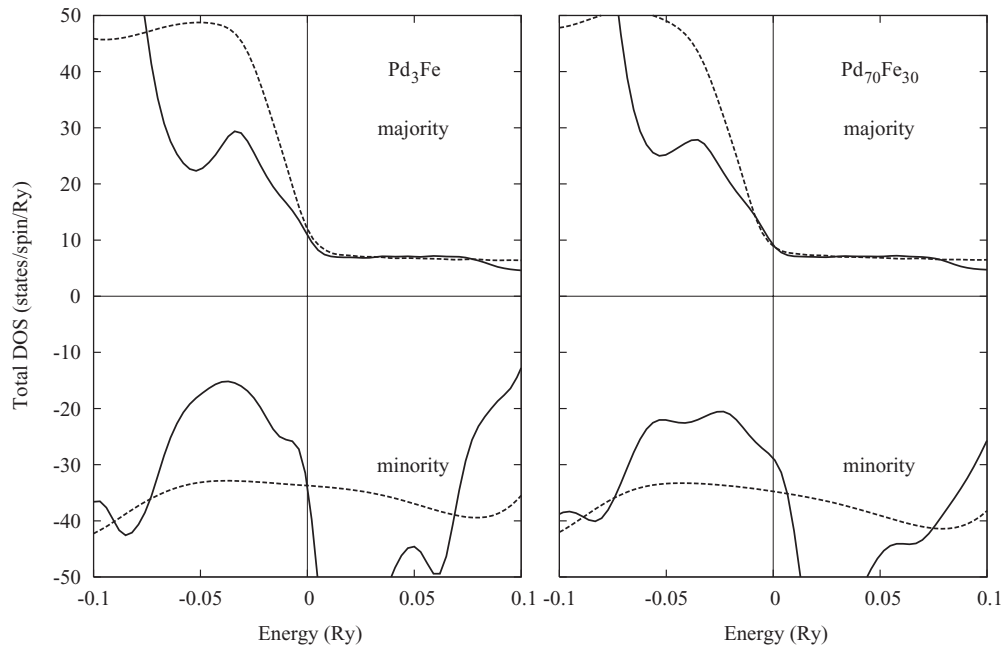


FIG. 3. The relativistic spin-resolved ferromagnetic total densities of states for most ordered (full lines) and fully disordered (dashed lines) phases of Pd₃Fe and Pd₇₀Fe₃₀ alloys in the energy window around the Fermi energy. The Fermi energy is set to zero.

in Figs. 4 and 5 for Pd₃Fe and Pd₇₀Fe₃₀ alloys, respectively. The local Fe moment around 3 μ_B depends only weakly on varying environment in all cases. The local Pd moment around 0.45 μ_B is almost constant on its own sublattice, but it drops almost to zero on the Fe sublattice, where it is surrounded mainly by Pd atoms. These results are in a good agreement with experiment.²² It should be noted that Fe atoms are on the simple cubic sublattice, which is rather unusual as compared to bcc-like Fe (moment about 2.2 μ_B), or to fcc-like Fe

in Heusler- or D0₃-based alloys. For example, Fe moments around 1.85–2.3 μ_B are found in Fe₃Al alloy²³ while Fe₂VAl Heusler alloy is nonmagnetic.²³ A strong dependence on chemical order is found in FeAl alloy: its ordered CsCl phase is paramagnetic, but its disordered phase is ferromagnetic.²⁴ This is due to the occurrence of bcc-like coupling among Fe atoms on disordered lattice as contrasted with sc-like coupling

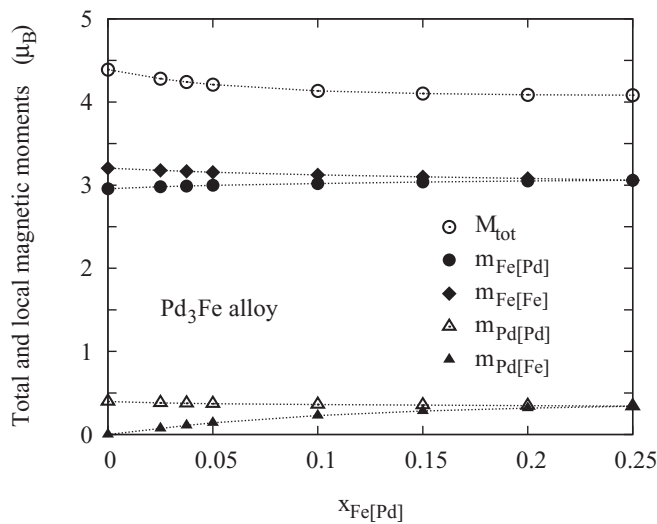


FIG. 4. The total and component-resolved magnetic moments for partly ordered Pd₃Fe alloys. The amount of possible antisite disorder in the system is measured by concentration $x_{\text{Fe}[\text{Pd}]}$ of Fe atoms on Pd sublattices. The cases $x_{\text{Fe}[\text{Pd}]} = 0$ and $x_{\text{Fe}[\text{Pd}]} = 0.25$ correspond to a fully ordered Pd₃Fe alloy and to a completely disordered fcc-Pd₇₅Fe₂₅ alloy, respectively.

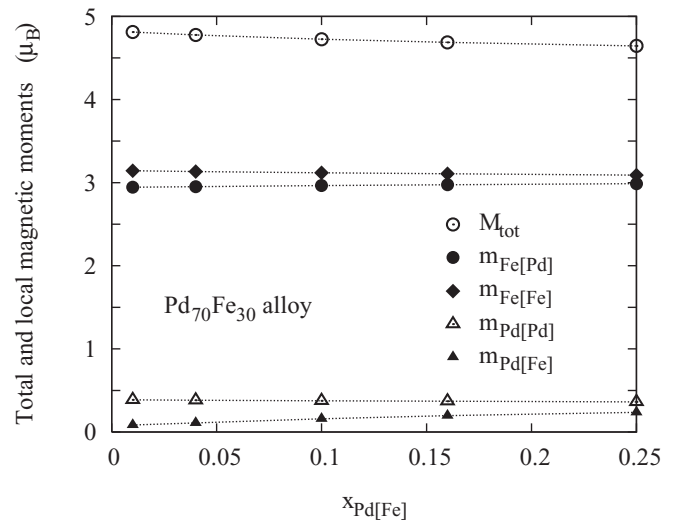


FIG. 5. The same as in Fig. 3 but for the nonstoichiometric Pd₇₀Fe₃₀ alloy. In this case we measure the amount of disorder via the concentration $x_{\text{Pd}[\text{Fe}]}$ of Pd atoms on the Fe sublattice. This choice assumes that the most ordered case represents the model with fully occupied Fe sublattice, while the surplus Fe atoms are distributed randomly on three Pd sublattices. The completely disordered alloy corresponds to $x_{\text{Pd}[\text{Fe}]} = 0.7$ on each of four sublattices. The total and local magnetic moments for $x_{\text{Pd}[\text{Fe}]} = 0.4, 0.55,$ and 0.7 (not shown) are almost identical to those corresponding to $x_{\text{Pd}[\text{Fe}]} = 0.25$.

with enlarged distance in ordered CsCl phase. On the contrary, in ordered FeRh alloy with CsCl structure Fe moments are also on the simple cubic lattice, but Rh atoms carry a large induced moment and strong Fe-Rh coupling is responsible for a large Fe moment around $3 \mu_B$.^{25,26} However, the magnetism in this system is very complex and we refer the reader to a recent study.²⁷ All this illustrates is the sensitivity of the Fe moment to the structural and chemical environment.

In addition to a relativistic study, we have performed scalar-relativistic calculations for a few samples. In general, very good agreement between both relativistic and scalar-relativistic calculations was obtained for spin moments. The total orbital moment was almost the same for all systems varying between 0.15 and 0.17 μ_B per formula unit.

B. Residual resistivity and AMR ratio

The resistivities of Pd₃Fe and Pd₇₀Fe₃₀ alloys as functions of antisite concentrations are shown in Fig. 6. Calculations correspond to the temperature $T = 0$ K and should be compared to experimental results for $T = 4.2$ K.⁶ In the case of Pd₃Fe alloy we interpolate between perfectly ordered and disordered phases. It should be noted that the completely disordered Pd₇₀Fe₃₀ alloy corresponds to $x_{\text{Pd}[\text{Fe}]} = 0.7$. We found a maximum of the resistivity around $x_{\text{Fe}[\text{Pd}]} = 0.1$ for Pd₃Fe.

We found a monotonic increase of the resistivity with Pd-antisite disorder on the Fe-lattice for Pd₇₀Fe₃₀ in the concentration range shown in Fig. 6. Resistivities for higher concentrations ($x_{\text{Pd}[\text{Fe}]} = 0.4, 0.55,$ and 0.7) are similar and exhibits only a very shallow maximum (not shown, cf. Fig. 8). The calculated resistivities are found in the range observed in the experiment which is between 5 and 15 $\mu\Omega$ cm for differently annealed samples.⁶ The differences in behavior of both alloy systems result from different electron concentrations and different behavior of electron states at the Fermi energy as

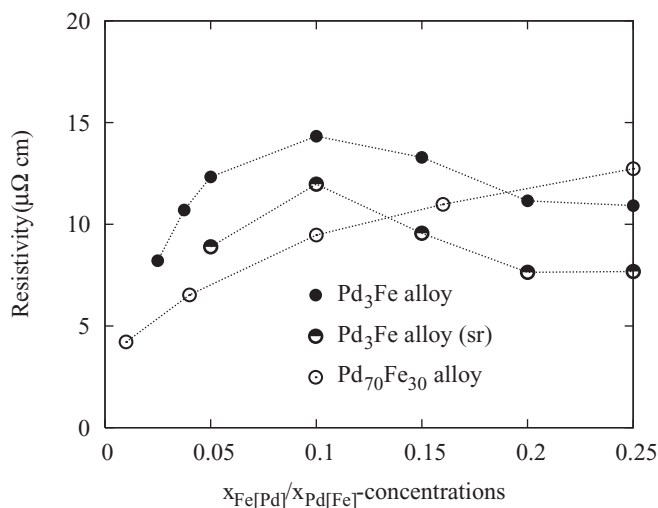


FIG. 6. Resistivity as a function of possible disorder characterized by antisite Fe concentration on Pd sublattices (stoichiometric Pd₃Fe alloy) and by antisite Pd concentration on the Fe sublattice (nonstoichiometric Pd₇₀Fe₃₀ alloy). Scalar-relativistic (sr) resistivity without spin-orbit coupling is also shown for Pd₃Fe alloy.

indicated by Fig. 3. It should be noted that the effect of vertex corrections is nonnegligible due to dominating d scatterings (cf. Fig. 9 below).

For Pd₃Fe alloy we also show corresponding resistivities obtained by the scalar-relativistic counterpart of Eq. (1). The following conclusions can be made: (i) in the scalar-relativistic case the current is conducted by majority and minority states independently (two-current model). The minority states are influenced by disorder more strongly as compared to majority ones (see Fig. 2). As a result, the conductivity is dominated by the majority channel (an order of magnitude larger as compared to the minority channel). (ii) The spin-orbit coupling mixes up both channels and increases the total resistivity. (iii) The effect of vertex corrections is nonnegligible. They reduce the total resistivity by about 20%.

A more detailed comparison with the experiment can be obtained by plotting the AMR vs resistivity, which is done in Fig. 7 for Pd₃Fe and in Fig. 8 for Pd₇₀Fe₃₀. Two branches found for the Pd₃Fe system are due to the maximum of the resistivity as a function of disorder. The lower branch exhibits a weak dependence of AMR vs resistivity with values of the AMR around 4.5% which seems to agree reasonably well with experiment. On the other hand, at least the AMR values corresponding to almost completely disordered samples have higher AMR than those found in the experiment although covering similar resistivity range. One can therefore speculate that the measured samples are not completely disordered. Even better agreement between theory and experiment⁶ is obtained for the nonstoichiometric Pd₇₀Fe₃₀ case. The AMR decreases with increasing resistivity (disorder) in agreement with experiment and also quantitative agreement for both the AMR and resistivity is satisfactory. The resistivities and AMR for disordered samples ($x_{\text{Pd}[\text{Fe}]} = 0.4, 0.55,$ and 0.7) shown in Fig. 8 with half-filled symbols are similar to each other. This seems to indicate, similarly to the case of Pd₃Fe, that samples

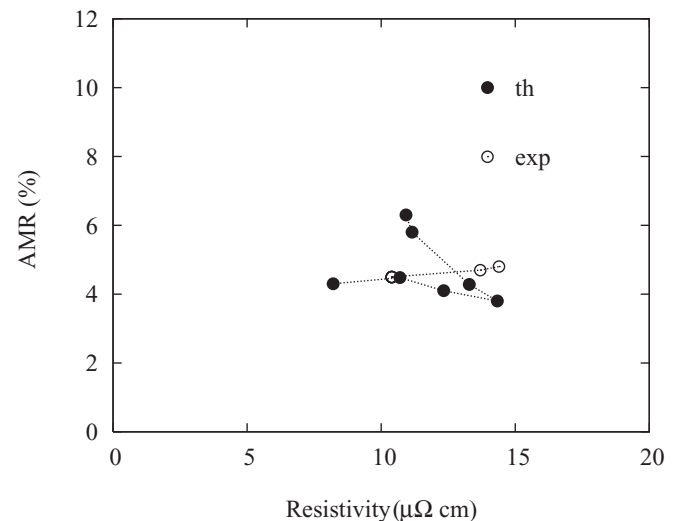


FIG. 7. The calculated AMR vs resistivity (th) for the stoichiometric Pd₃Fe alloy with a possible antisite disorder compared with experimental data (exp) of Ref. 6. Two branches obtained in the theoretical simulation are marked by the maximum of the resistivity as a function of antisite Fe concentration (see Fig. 6). The bottom branch corresponds to smaller antisite concentrations.

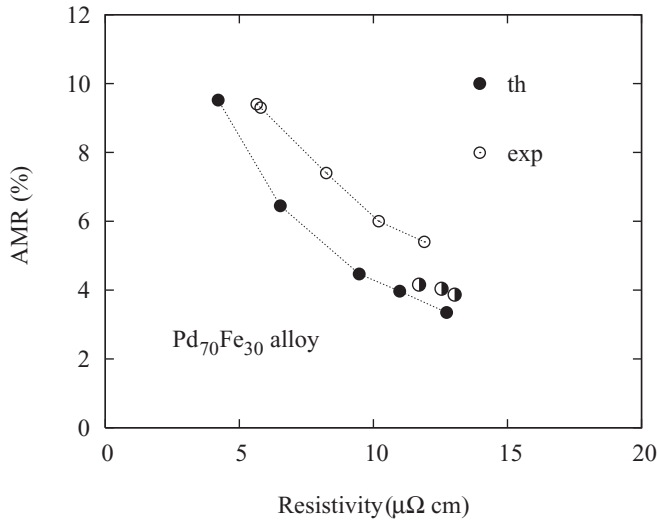


FIG. 8. The same as in Fig. 7 but for the nonstoichiometric $\text{Pd}_{70}\text{Fe}_{30}$ case. See Fig. 6 for resistivities and corresponding values of antisite disorder. Half-filled symbols correspond to disordered samples with $x_{\text{Pd}[\text{Fe}]} = 0.4, 0.55, \text{ and } 0.7$.

with a smaller amount of disorder correspond to annealed samples used in the experiment.

We can conclude that in agreement with experiment we have obtained different behavior of Pd_3Fe and $\text{Pd}_{70}\text{Fe}_{30}$ samples, namely weak dependence on the disorder in the former and pronounced dependence in the latter cases. Such behavior can be traced down to a different number of carriers and different behavior of electronic states at the Fermi energy (transport relaxation time and velocities) which both influence the transport properties.

It should be noted that even better agreement with experiment for both systems can be obtained assuming a small residual resistivity of order $1\text{--}2 \mu\Omega \text{ cm}$. It is most probably due to some amount of antisite Fe atoms on Pd sublattice, although the presence of foreign impurities as well as some amount of the short-range order which is not captured by the present CPA treatment are also possible. To verify this assumption we have calculated the Pd_3Fe alloy containing very small concentration of Fe antisites. We found that the residual resistivity of order $2 \mu\Omega \text{ cm}$ is obtained for the antisite concentration $x_{\text{Fe}[\text{Pd}]} = 0.005$.

C. Temperature dependence of AMR

The temperature in general enhances resistivities of metallic systems. In magnetic alloys are two relevant mechanisms: (i) scattering on phonons which leads to a linear increase of the resistivity with temperature T (with exception of very low T), and (ii) scattering on magnons (spin disorder resistivity) which leads in typical magnetic metals to an increase of the resistivity $\propto (T/T_c)^2$ below magnetic Curie temperature T_c and to a saturated constant value for higher T , where the magnetic short-range effect has vanished.⁸ More precisely, the resistivity due to spin disorder is constant in the thermodynamic limit in which spin-spin correlations vanish. This state of thermodynamic spin disorder can be simulated by the DLM approach⁹. We have verified that the DLM

resistivity of bcc Fe indeed agrees quite well with both the experiment and existing theory, thus indicating a dominating character of spin disorder over contribution from phonons with the exception of very low temperatures.²⁸ The DLM model can be straightforwardly incorporated into the transport CPA formalism. In this model the spin disorder is simulated by a concentrated alloy of collinear spins pointing in opposite directions and treated self-consistently in the framework of the CPA.⁹ We note that the situation is less clear for smaller T below the thermodynamical limit (below Curie temperature) in which still exists a global magnetization although with a reduced magnitude as compared to the case with $T = 0 \text{ K}$. The simplest picture which simulates this situation, at least qualitatively, is the uncompensated DLM (uDLM) state in which “concentrations” of oppositely oriented spins are different. We will characterize this spin disorder by the ratio $r = x[-] : x[+]$, where $x[-]$ is the concentration of oppositely oriented moments. In the limit when $r = 0$ we recover the ferromagnet at $T = 0 \text{ K}$ while $r = 1$ corresponds to the DLM state. In general it is impossible to relate reliably concentrations of spins in the uDLM state with a specific temperature, although it is tempting to correlate them with theoretical (experimental) temperature dependence of sample magnetization.²⁹ Although a simple procedure of mapping of spin concentrations in the partial DLM state to the reduced temperature T/T_c was described in the literature,³⁰ in particular for Fe-Pt Invar alloys, they are essentially phenomenological and may be regarded only as a semiquantitative way to trace continuous changes of some physical properties. We mention that a simple model theory of spin disorder resistivity for dilute PdFe alloys (Fe concentrations less than 1%, the giant-magnetic moment regime) was developed in Ref. 31.

Our task in this section is merely to understand a fast increase/decrease of the resistivity/AMR ratio with temperature and thus make at least qualitative conclusions based on first-principle uDLM calculations. Since the room temperature, where AMR ratio has been measured, is much smaller than experimental Curie temperatures of Pd-Fe alloys (about 540 K), one could expect that the spin disorder in the region of interest can be represented with relatively small number of atoms with down moments in the uDLM state. Indeed, as it will be seen below, already $r = 1 : 19$ ratio of down moments to up moments leads to the experimentally observed reduction of the AMR ratio and enhanced resistivity.⁶ This fact and the above discussed bcc-Fe case allow us to speculate that the main mechanism leading to decrease of the AMR ratio and increase of resistivity at room temperatures are thermal spin disorder effects. This conclusion is in an agreement with a proposal made by authors of the experimental study of the electrical resistivity of PdFe alloys.³²

We have chosen as a case study $\text{Pd}_{70}\text{Fe}_{30}$ with 10% of Pd[Fe] antisites ($x_{\text{Pd}[\text{Fe}]} = 0.1$). The uDLM was applied to Fe spins both on Fe and Pd sublattices (small local moments on Pd atoms collapse in the DLM state).

The results are summarized in Table I in which the effect of temperature corresponds to an increasing amount of oppositely oriented spins: the ferromagnet, or the $T = 0 \text{ K}$ limit corresponds to the case without oppositely oriented spins, the equiconcentration case corresponds to the DLM, or T above the Curie temperature (about 540 K for Pd_3Fe). Results

TABLE I. The electronic (total magnetization M_{tot}) and transport (resistivity ρ and AMR properties of $\text{Pd}_{70}\text{Fe}_{30}$ alloy with 10% of $\text{Pd}[\text{Fe}]$ antisites as a function of spin disorder characterized by the ratio $r = x[-] : x[+]$ of oppositely oriented spins in the framework of uncompensated DLM model). The amount of spin disorder increases from $r = 0$ (ferromagnetic state, FM, no disorder) to $r = 1$ (DLM state, full disorder).

$r = x[-] : x[+]$	$\text{Pd}_{70}\text{Fe}_{30}$ with 10% of $\text{Pd}[\text{Fe}]$ antisites		
	M_{tot} (μB)	ρ ($\mu\Omega\text{ cm}$)	AMR (%)
0 (FM)	4.73	9.47	4.47
1:39	4.49	29.85	0.97
1:19	4.26	44.59	0.47
1:9	3.79	65.56	0.26
2:5	1.99	100.81	0.06
1:1 (DLM)	0.0	109.26	0.0

for $T = 4.2$ and 77 K are rather similar⁶ indicating thus a negligible spin disorder. Our resistivity for $r = 0$ ($9.47 \mu\Omega\text{ cm}$) roughly corresponds to the experimental value of $8.24 \mu\Omega\text{ cm}$ for $T = 4.2$ K which rises to value around $50 \mu\Omega\text{ cm}$ for $T = 295$ K. This corresponds roughly to our case $r = 1 : 19$ in Table I and the reduction of the AMR from 4.47% to 0.47% agrees fairly well with experimental data (AMR drops from 6% to 0.45%). It should be noted that reduction of the total magnetization is small for this case, which is in agreement with the fact that we are still far from the Curie point. We can conclude that the spin disorder is mostly responsible for a strong increase/reduction of the resistivity/AMR observed in the experiment with increasing T . Also the order of these changes falls within the experimental range.

D. Anomalous Hall effect

Here we present results for the AHE as a function of order in the system. To this end we show in Fig. 9 the AHE vs resistivity for both studied systems. We also show results for the coherent part of the AHE which can be roughly identified with the *intrinsic* part of the AHE (see discussion at the end of Sec. II). The following conclusions can be made: (i) The effect of vertex corrections on the total resistivity is nonnegligible and leads to its reduction. (ii) We observe only a weak dependence of the intrinsic part of the AHE on the resistivity (i.e., on impurity disorder). This is consistent with the assumption that the coherent part of the AHE is dominated by intrinsic contribution. (iii) A noticeable feature is the change of the sign of the AHE when the disorder in the system increases, indicating increasing role of the skew scattering. This result is in a qualitative agreement with experiment for fcc-PdFe, PdNi, and PdCo alloys,³³ although in the present case it corresponds to a various amount of disorder due to thermal annealing and not to the change of alloy composition. The direct comparison of calculated AHE with the most disordered phases of Pd_3Fe and $\text{Pd}_{70}\text{Fe}_{30}$ alloys is complicated by the fact that in this concentration region is experimentally observed the sign change.³³ Our $\text{AHE} = -7.5$ kS/m is inbetween the experiment³³ and recent relativistic KKR-CPA theory¹⁶ for the most disordered phase of $\text{Pd}_{70}\text{Fe}_{30}$. A reasonable agreement between the present and KKR theory¹⁶ is also obtained for

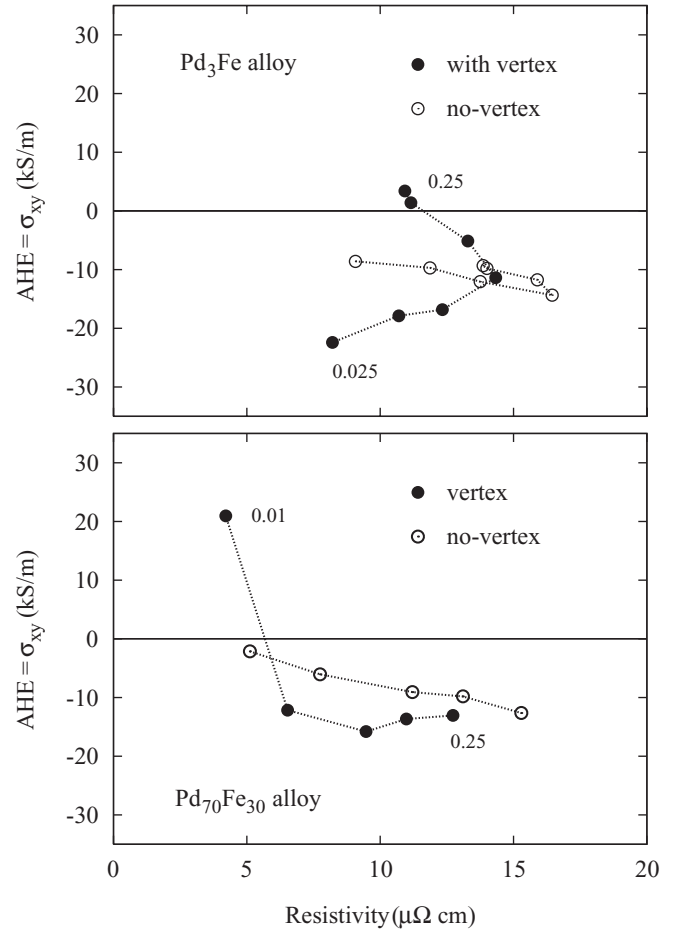


FIG. 9. The calculated AHE vs resistivity for the stoichiometric (Pd_3Fe) and for the nonstoichiometric ($\text{Pd}_{70}\text{Fe}_{30}$) alloys. Full/empty symbols denote full calculations/coherent part only in which the vertex corrections are neglected. Numbers indicate the smallest/largest values of corresponding impurity concentrations. For a detailed relation between concentrations and resistivities see Fig. 6.

pure bcc Fe: -55 and 64 kS/m, respectively, while experiment gives 105 kS/m. It should be noted that due to different definitions the present values of the AHE for bcc-Fe and fcc-PdFe alloys have consistently opposite signs as compared to Ref. 16. Finally, assuming that the dominating temperature effect on the AHE is again the spin disorder like for the AMR, and assuming the same model as in Table I, we have found a strong reduction of the AHE value by the spin disorder. We have obtained $\text{AHE} = -16$ kS/m for $T = 0$ ($r = 0$) to $\text{AHE} = -5.6$ kS/m for $r = 1 : 19$ and AHE is zero in the paramagnetic state ($r = 1 : 1$).

IV. CONCLUSIONS

We have presented first-principles study of magnetotransport properties of Pd-rich PdFe alloys as a function of the order in the system which is due to different temperature treatments of studied samples. Our calculations are based on the relativistic generalization of the linear-response theory (Kubo-Greenwood formula) as implemented in the framework of the TB-LMTO-CPA approach and they allowed us to

relate the amount of order in the system with the resistivity. This relation can be employed as a complementary tool to conventional x-ray and neutron-scattering experiments used to determine the amount of order in the system. The results agree reasonably well with experimental data for both stoichiometric Pd₃Fe and for nonstoichiometric Pd₇₀Fe₃₀ alloys.⁶ In particular, not only the trends but also magnitudes of the resistivity and the AMR agree reasonably well. Small differences in electron concentrations are origin of different experimentally observed trends in AMR vs resistivity curves, namely the AMR is essentially constant with respect to increased disorder for Pd₃Fe alloys and it markedly decreases with disorder for Pd₇₀Fe₃₀ alloys. We have also predicted behavior of the AHE as a function of the order in the system. A detailed comparison with experiment and theory¹⁶ in the limit of the completely disordered fcc-Pd₇₅Fe₂₅ alloy is complicated by an experimentally observed crossover between positive and negative AHE which occurs in this concentration region.

Finally, we have also discussed the effect of temperature on magnetotransport properties using the uncompensated DLM approach. Present calculations do not allow us to relate magnetotransport properties with a specific temperature reliably, nevertheless a qualitative and to some extent also quantitative agreement with trends observed in the experiment was obtained. Results of calculations allow us to make the conclusion that the spin disorder is mostly responsible for strong increase (reduction) of the resistivity (AMR ratio) with temperature found in experiment.

ACKNOWLEDGMENTS

The authors acknowledge the financial support from AV0Z 10100520 (J.K. and V.D.), AV0Z 20410507 (I.T.), and from the Czech Science Foundation (P204/11/1228). S.K. acknowledges support from Austrian OEFG within MOEL program (No. 500).

-
- ¹R. L. Rossiter, *The Electrical Resistivity of Metals and Alloys* (Cambridge University Press, Cambridge, London, 1987).
- ²P. Weinberger, *Phys. Rep.* **377**, 281 (2003).
- ³J. Banhart and H. Ebert, *Europhys. Lett.* **32**, 517 (1995).
- ⁴S. Khmelevskiy, K. Palotas, L. Szunyogh, and P. Weinberger, *Phys. Rev. B* **68**, 012402 (2003).
- ⁵J. Banhart and G. Czycholl, *Europhys. Lett.* **58**, 264 (2002).
- ⁶Y. Hsu, S. Jen, and L. Berger, *J. Appl. Phys.* **50**, 1907 (1979).
- ⁷J. M. Ziman, *Electrons and Phonons* (Oxford University Press, Oxford, 1960).
- ⁸T. Kasuya, *Prog. Theor. Phys.* **16**, 58 (1956).
- ⁹B. L. Gyorffy, A. J. Pindor, J. Staunton, G. M. Stocks, and H. Winter, *J. Phys. F: Metal Phys.* **15**, 1337 (1985).
- ¹⁰P. R. Tulip, J. B. Staunton, S. Lowitzer, D. Ködderitzsch, and H. Ebert, *Phys. Rev. B* **77**, 165116 (2008).
- ¹¹O. K. Andersen and O. Jepsen, *Phys. Rev. Lett.* **53**, 2571 (1984).
- ¹²I. Turek, V. Drchal, J. Kudrnovský, M. Šob, and P. Weinberger, *Electronic Structure of Disordered Alloys, Surfaces and Interfaces* (Kluwer, Boston, 1997).
- ¹³S. H. Vosko, L. Wilk, and M. Nusair, *Can. J. Phys.* **58**, 1200 (1980).
- ¹⁴I. Turek, V. Drchal, and J. Kudrnovský, *Philos. Mag.* **88**, 2787 (2008).
- ¹⁵A. Crépieux and P. Bruno, *Phys. Rev. B* **64**, 014416 (2001).
- ¹⁶S. Lowitzer, D. Ködderitzsch, and H. Ebert, *Phys. Rev. Lett.* **105**, 266604 (2010).
- ¹⁷I. Turek and T. Záležák, *J. Phys.: Conf. Ser.* **200**, 052029 (2010).
- ¹⁸I. Turek, J. Kudrnovský, and V. Drchal, e-print [arXiv:1111.4793](https://arxiv.org/abs/1111.4793) (to be published).
- ¹⁹I. Turek, J. Kudrnovský, V. Drchal, L. Szunyogh, and P. Weinberger, *Phys. Rev. B* **65**, 125101 (2002).
- ²⁰K. Carva, I. Turek, J. Kudrnovský, and O. Bengone, *Phys. Rev. B* **73**, 144421 (2006).
- ²¹C. A. Kuhnen and E. Z. da Silva, *J. Magn. Magn. Mater.* **67**, 260 (1987); S. K. Bose, J. Kudrnovský, M. van Schilfgaarde, P. Bloechl, O. Jepsen, M. Methfessel, and A. T. Paxton, *ibid.* **87**, 97 (1990).
- ²²J. W. Cable, E. O. Wollan, and W. C. Koehler, *Phys. Rev.* **138**, A755 (1965).
- ²³B. Xu, J. Liu, and L. Yi, *Phys. Lett. A* **363**, 312 (2007).
- ²⁴J. Fässbender, M. O. Liedke, T. Strache, W. Möller, E. Menéndez, J. Sort, K. V. Rao, S. C. Deevi, and J. Nogués, *Phys. Rev. B* **77**, 174430 (2008).
- ²⁵G. Shirane, R. Nathans, and C. W. Chen, *Phys. Rev.* **134**, A1547 (1963).
- ²⁶V. L. Moruzzi and P. M. Marcus, *Phys. Rev. B* **46**, 14198 (1992); I. Turek, J. Kudrnovský, V. Drchal, P. Weinberger, and P. H. Dederichs, *J. Magn. Magn. Mater.* **240**, 162 (2002).
- ²⁷L. M. Sandratskii and P. Mavropoulos, *Phys. Rev. B* **83**, 174408 (2011).
- ²⁸A. L. Wysocki, R. F. Sabirianov, M. van Schilfgaarde, and K. D. Belashenko, *Phys. Rev. B* **80**, 224423 (2009).
- ²⁹S. K. Bose, J. Kudrnovský, V. Drchal, and I. Turek, *Phys. Rev. B* **82**, 174402 (2010).
- ³⁰S. Khmelevskiy, I. Turek, and P. Mohn, *Phys. Rev. Lett.* **91**, 037201 (2003).
- ³¹N. C. Koon, A. I. Schindler, and D. L. Mills, *Phys. Rev. B* **6**, 4241 (1972).
- ³²S. Skalski, M. P. Kawatra, J. A. Mydosh, and J. I. Budnick, *Phys. Rev. B* **2**, 3613 (1970).
- ³³V. A. Matveev and G. V. Fedorov, *Fiz. Met. Metalloved.* **53**, 34 (1982).